Gas-Phase Reactions

DOI: 10.1002/anie.201104433

C–N and C–C Bond Formations in the Thermal Reactions of "Bare" $Ni(NH_2)^+$ with C_2H_4: Mechanistic Insight on the Metal-Mediated Hydroamination of an Unactivated Olefin**

*Robert Kretschmer, Maria Schlangen, and Helmut Schwarz**

In memory of Emanuel Vogel

The central role of nitrogen-containing compounds in biological and in in vitro systems is reflected in ongoing research to improve currently employed synthetic methods for the production of this important class of substances.[1] An atom-economic process, using simple starting materials and producing no or only negligible side products, involves the addition of the N–H bond of ammonia across carbon–carbon multiple bonds, the so called hydroamination.[2] In its simplest form, that is, for the couple C_2H_4/NH_3, the reaction exhibits a free enthalpy of reaction of about -17 kJ mol^{-1} but does not proceed under ambient conditions because the electrostatic repulsion of the nitrogen electron lone pair and the relatively electron-rich double bond of the olefin results in a rather high activation barrier.[3] Further, a conceivable [2+2] cycloaddition is unfavorable owing to the significant HOMO/LUMO energy gaps of the respective N–H and C=C orbitals, not to speak of the symmetry forbidden nature of a concerted reaction (Figure 1).[2a,3,4] To circumvent these obstacles, catalysts have been employed for the hydroamination of olefins, and remarkable efforts have been undertaken in the last two decades aimed at developing an effective catalytic route.[5] There are two general approaches in this context: activation of either the olefin or of the N–H bond.[2c] In the former strategy, which corresponds to the oldest class of hydroamination, an alkene first coordinates to an electrophilic metal center followed by a nucleophilic attack of the amine to the polarized olefin. In the latter approach, which is limited to a few examples, the hydrocarbon coordinates to the metal center of an amide complex and C–N bond coupling is achieved by migratory insertion of the alkene into the M–N bond, resulting in the formation of an aminoalkyl intermediate.[6] Further, both the inter- and intramolecular variants of the hydroamination can be catalyzed by for example, alkali metals,[7] late transition metals,[8] as well as lanthanides and actinides.[9] Notwithstanding all progress, the intermolecular hydroamination of unactivated olefins using simple amines remains quite challenging.[10] However, a metal-free hydroamination of ethylene by ammonia was recently observed using an electron beam impinging on C_2H_4/NH_3 multilayer films.[11] Quite clearly, for the development of efficient catalysts, knowledge of the elementary steps of a cycle as well as insight in the intrinsic properties of the active catalytic centers are indicated. As demonstrated before for various C–N coupling processes,[12] catalytically active intermediates, which are otherwise not accessible under more conventional conditions, can be identified by means of gas-phase experiments and have strongly gained in importance during the last decades.[13]

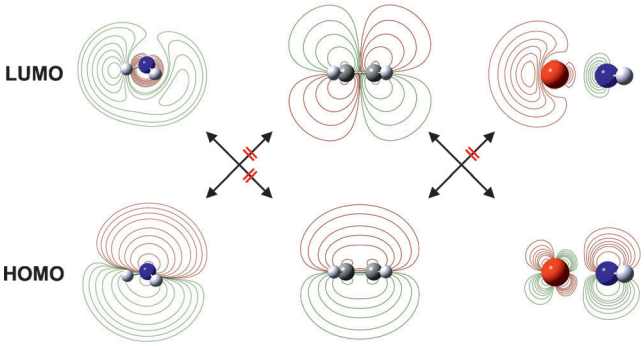

Figure 1. HOMO and LUMO contour plots for NH_3, C_2H_4, and $Ni(NH_2)^+$ generated by using Gaussian09 at the UB3LYP/def2-QZVP level of theory.

Herein, we report the gas-phase thermal ion/molecule reactions of the "bare" amidonickel cation, $Ni(NH_2)^+$, which can be easily generated in the gas phase by reacting $Ni(OH)^+$ with ammonia[14] or by collision-induced dissociation of $Ni(formamide)_3^{2+}$.[15] In addition to the outstanding position that ligated nickel ions occupy in gas-phase reactions,[16] nickel compounds exhibit a large versatility in chemical and enzymatic reactions.[17]

As shown in Figure 2, the thermal reaction of mass-selected $Ni(NH_2)^+$ with ethylene results in the formation of two primary products [Equations (1) and (2)], with a branch-

[*] Dipl.-Chem. R. Kretschmer, Dr. M. Schlangen, Prof. Dr. H. Schwarz
Institut für Chemie, Technische Universität Berlin
Strasse des 17. Juni 135, 10623 Berlin (Germany)
E-mail: Helmut.Schwarz@mail.chem.tu-berlin.de
Prof. Dr. H. Schwarz
Department of Chemistry, Faculty of Science, King Abdulaziz University
P. O. Box 80203, Jeddah 21589 (Saudi Arabia)
E-mail: HSchwarz@kau.edu.sa

[**] Financial support from the Cluster of Excellence "Unifying Concepts in Catalysis" (EXC 314/1) funded by the Deutsche Forschungsgemeinschaft and administered by the Technische Universität Berlin is gratefully acknowledged. We appreciate helpful discussions with Lena Kleineidam and are grateful to the referees for critical comments and suggestions. R.K. acknowledges the Stiftung Stipendien Fonds des Verbandes der Chemischen Industrie for a Kekulé scholarship.

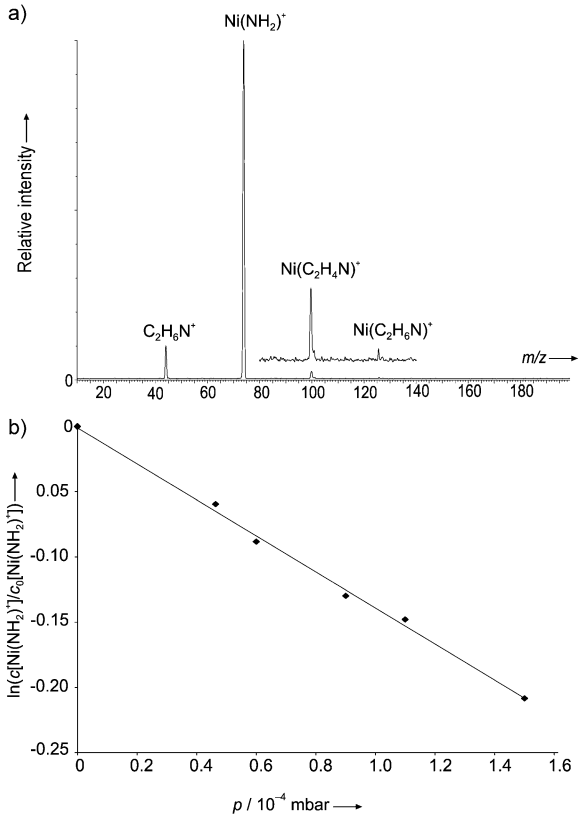

Figure 2. a) Mass spectrum resulting from thermal ion/molecule reactions of mass-selected $Ni(NH_2)^+$ with ethylene at a pressure of 0.9×10^{-4} mbar (the region between *m/z* 80 and 140 is enlarged by a factor of 10); b) Plot of $\ln(c[Ni(NH_2)^+]/c_0[Ni(NH_2)^+])$ versus ethylene pressure *p*.

$$Ni(NH_2)^+ + C_2H_4 \rightarrow C_2H_6N^+ + Ni \quad (1)$$

$$Ni(NH_2)^+ + C_2H_4 \rightarrow Ni(C_2H_4N)^+ + H_2 \quad (2)$$

ing ratio of 3.1:1[18] and with a rate coefficient of $(1.9\pm0.95)\times10^{-10}\,cm^3\,s^{-1}\,molecule^{-1}$. The reaction is facile and proceeds with an efficiency of $(18\pm9)\%$ relative to the gas-kinetic collision limit ($10.7\times10^{-10}\,cm^3\,s^{-1}$ molecule^{-1}).[19] Adequate thermalization of the $Ni(NH_2)^+$ ion is indicated by the linear decrease of its abundance as a function of ethylene pressure (Figure 2b).

The ion $C_2H_6N^+$ (*m/z* 44) is often observed as a prominent signal in the mass spectra of amines, and *N*-protonated ethylideneamine was found to be the most stable species of all chemically conceivable isomers.[20] Additionally, a secondary reaction according to Equation (3) takes place; as expected

$$Ni(C_2H_4N)^+ + C_2H_4 \rightarrow Ni(C_4H_6N)^+ + H_2 \quad (3)$$

for such a process, reaction (3) gains in importance at higher ethylene pressure. The assignment of reaction (3) with $Ni(C_2H_4N)^+$ serving as a reactive intermediate is further supported by its decrease at higher C_2H_4 pressure. Secondary reactions of ethylene including C–C bond coupling have already been observed for $Y(NH)^+$, yielding $Y(C_4H_5N)^+$ and H_2;[12b] further, organometallic complexes that contain Ni, Pd, or Pt as metal cores serve as catalysts for the telomerization of dienes in the presence of an appropriate nucleophile, such as NH_3.[21]

The assignments of these reaction channels [Equations (1)–(3)] are in keeping with labeling experiments, in which *E*- and *Z*-CHDCHD as well as C_2D_4 have been employed.[22] While these time-honored labeling experiments do not provide direct mechanistic insight for reaction (1), interesting aspects are provided as to the origin of molecular hydrogen formed in processes (2) and (3). For example, H_2 generated in reaction (2) contains one hydrogen atom from ethylene and one from the amide group; in contrast, in the formation of the second molecule of hydrogen [Equation (3)], N–H bond activation is not involved; rather, the incoming substrate serves as the sole source for the elimination of molecular hydrogen. Further, an intramolecular kinetic isotope effect (KIE), $k_H/k_D = 1.4$, has been determined for reaction (2) by investigating the ion/molecule reactions of $Ni(NH_2)^+$ with *E*- and *Z*-CHDCHD; there is no effect of the stereochemistry of the two $C_2H_2D_2$ stereoisomers on the KIE.

DFT calculations were performed to obtain mechanistic insight in the C–N coupling reactions [Equations (1) and (2)] as well as the C–C coupling process according to Equation (3). In Figure 3, the potential-energy surfaces (PESs) of the primary reactions for the ground and first excited state are depicted. The formation of *N*-protonated ethylidenamine and neutral atomic nickel [reaction (1)] is shown in the upper part. As other possible isomers of $C_2H_6N^+$, for example the ethene ammonium ion or the aziridinium ion are higher in energy by 68.9 kJ mol^{-1} and 99.9 kJ mol^{-1}, their involvements in reaction (1) are unlikely. Commencing with an electrophilic addition to form the adduct complex **1**, the carbon–metal and carbon–nitrogen bonds are then formed via the cyclic transition structure $\mathbf{TS}_{1/2}$ leading to intermediate **2**. In this process, an elongation of the ethylene C–C bond is involved; while complex **1** corresponds to a genuine nickel(II) ethylene complex,[23] the carbon–carbon bond in **2** is consistent with a C–C single bond and the C–C distance of $\mathbf{TS}_{1/2}$ is in between. Next, a sequence of two metal-mediated hydrogen-atom shifts occurs. The first proceeds via $\mathbf{TS}_{2/3}$ to generate the metal hydride species **3**, and then, passing through $\mathbf{TS}_{3/4}$, complex **4** is formed; the latter decomposes directly to neutral atomic nickel and *N*-protonated ethylideneamine. The alternative, charge-inversed dissociation of **3** to form ethylidenamine and NiH^+ is endothermic by 205.9 kJ mol^{-1} for the singlet and 130.6 kJ mol^{-1} for the triplet state of NiH^+; this discrimination is in line with the higher proton affinity $PA(C_2H_5N)$ (885 ± 8) kJ mol^{-1} compared to PA(Ni) (737 ± 8) kJ mol^{-1}.[24] Additionally, as shown in Figure 3b, complex **4** serves also as a precursor for the dehydrogenation to form $Ni(C_2H_4N)^+$. Insertion of the nickel atom in a N–H bond, via $\mathbf{TS}_{4/5}$, gives rise to the nickel hydride complex **5**. Molecular hydrogen is then generated in a σ-bond metathesis reaction via $\mathbf{TS}_{5/6}$ that possesses a coplanar Ni-C-H-H arrangement (dihedral angles 0.0° (singlet) and 7.7° (triplet), respectively), to yield complex **6**; elimination of H_2 from **6** completes the dehydrogenation path to produce the cationic product **7**, which is best described as a four-membered metallacycle. According to the calculations, the alternative formation of H_2

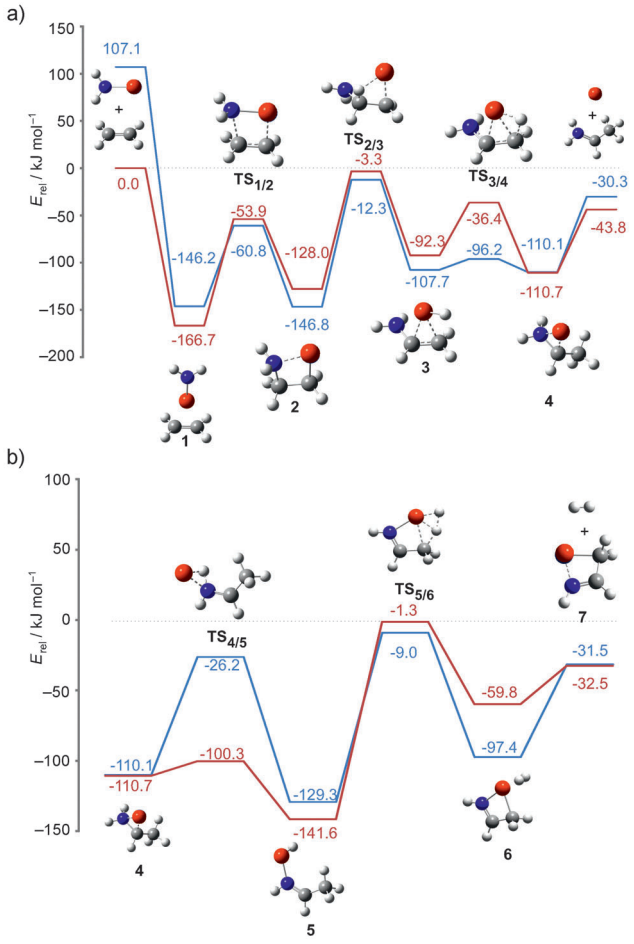

Figure 3. Simplified potential-energy surfaces of the $Ni(NH_2)^+/C_2H_4$ couple as calculated at the UB3LYP/def2-QZVP level of theory (singlet state is given in blue and triplet state is shown in red) for a) the formation of *N*-protonated ethylideneamine and atomic nickel [Equation (1)]; b) dehydrogenation leading to $Ni(CH_2CHNH)^+/H_2$ [Equation (2)]. For the sake of clarity, charges are omitted. C ●, H ●, N ●, Ni ●.

by N–H bond activation from intermediate **3** leading directly to **6** is prohibited by a barrier of 52.2 kJ mol^{-1} relative to the entrance channel. While the computational findings explain the labeling experiments well, they fail in accounting for the branching ratio of Equations (1) and (2). For example, according to the PESs shown in Figure 3, formation of $C_2H_6N^+$ [Equation (1)] should exceed the experimentally observed 3.1:1 ratio. This discrepancy may indicate some deficiency of the employed DFT functional in quantitatively correctly describing **TS**$_{4/5}$ and **TS**$_{5/6}$ (see also comments made in the Computational Section). Selected bond lengths of all intermediates and transition structures are given in Table 1; the geometries of *N*-protonated ethylideneamine and ethylene are in good agreement with published computational and experimental results, respectively.[20e,25] The role of the different spin states (singlet versus triplet) in the PESs will be addressed further below.

The metallacyclic complex $Ni(C_2H_4N)^+$ (**7**) reacts with a second molecule of ethylene. As shown in Figure 4, **7** forms with C_2H_4 an encounter complex **8**; the resulting structural changes with respect to the Ni–N and the ethylene C–C bonds are similar to those reported for complex **1**; that is, elongation of the Ni–N bond for the singlet versus contraction for the triplet state. The C–C bond of the incoming olefin is almost undisturbed for both states. Next, C–C bond coupling occurs by insertion of ethylene in the Ni–C bond (**TS**$_{8/9}$). Thus, a ring-expanded metallacycle **9** is generated in which the C–C bonds are close to the expected values of ordinary carbon–carbon single bonds. After a sequence of two hydrogen-atom transfers (originating selectively from C2 and C3) via **TS**$_{9/10}$ and **TS**$_{10/11}$, respectively, complex **11** is generated from which loosely bound molecular hydrogen is liberated. A conceivable hydrogen-atom transfer from the C1 position has been calculated to be endothermic for the singlet (43.5 kJ mol^{-1}) and triplet states (12.2 kJ mol^{-1}).[26] By comparing the geometrical parameters of **9** and **11**, the expected contraction of the C1-C2, C2-C3 and C3-C4 bonds is noted, which is due to a resonance-induced stabilization of the conjugated double

Table 1: Selected bond lengths (*r*), given in Å, of the species shown in Figure 3.[a]

	r(Ni–N)		*r*(Ni–C1)		*r*(C2–N)		*r*(C1–C2)		*r*(Ni–H)	
2S+1	1	3	1	3	1	3	1	3	1	3
$Ni(NH_2)^+$	1.721	1.825	–	–	–	–	–	–	–	–
C_2H_4	–	–	–	–	–	–	1.324[b]	–	–	–
1	1.825	1.792	2.174	2.205	2.174	2.205	1.355	1.354	–	–
TS$_{1/2}$	1.801	1.848	1.990	2.046	2.215	2.154	1.398	1.411	–	–
2	1.868	2.020	1.880	1.976	1.522	1.528	1.512	1.525	–	–
TS$_{2/3}$	2.654	3.400	1.898	1.964	1.443	1.346	1.487	1.492	1.783[c]	1.672[c]
3	2.129	2.116	2.011	2.474	1.386	1.420	1.391	1.345	1.437[c]	1.491[c]
TS$_{3/4}$	2.178	2.052	1.992	2.295	1.379	1.417	1.421	1.391	1.471[c]	1.567[c]
4	1.876	2.357	2.907	2.915	1.407	1.395	1.496	1.502	–	-
$C_2H_6N^+$	–	–	–	–	1.283	1.383	1.463	1.509	–	–
TS$_{4/5}$	1.829	1.952	3.366	3.357	1.322	1.283	1.468	1.48	1.648[d]	1.552[d]
5	1.828	1.958	3.315	3.342	1.282	1.282	1.473	1.474	1.418[d]	1.503[d]
TS$_{5/6}$	1.935	1.949	2.056	2.664	1.272	1.285	1.502	1.456	1.487c)	1.615c)
6	1.881	2.013	1.935	1.994	1.275	1.279	1.483	1.487	–	–
7	1.849	1.994	1.916	2.007	1.273	1.279	1.487	1.488	–	–

[a] The numbering is based on **TS**$_{1/2}$. C1 corresponds to the carbon atom directly bound to the nickel atom while C2 is connected with the nitrogen atom. [b] exp.: 1.337 Å, Ref. [25a]; [c] Ni–H bond of the hydrogen atom that migrates in **TS**$_{2/3}$; [d] Ni–H bond of the hydrogen atom that migrates in **TS**$_{4/5}$.

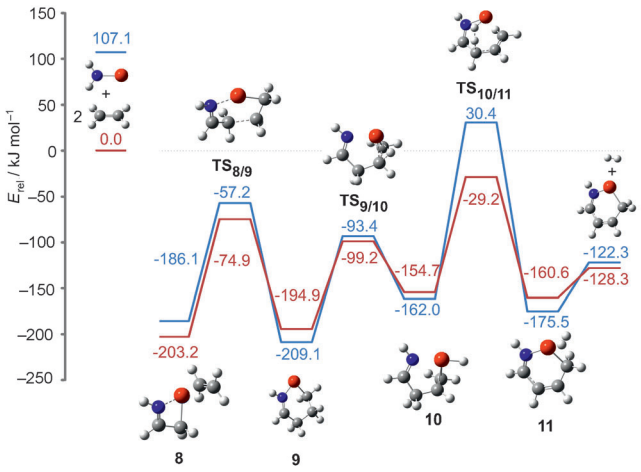

Figure 4. Simplified potential-energy surfaces of the secondary reaction of $Ni(NH_2)^+$ with C_2H_4 as calculated at the UB3LYP/def2-QZVP level of theory (singlet state is given in blue and triplet state is shown in red) for the dehydrogenation [Equation (3)]. For the sake of clarity, charges are omitted. C ●, H ●, N ●, Ni ●.

bonds. The elimination of molecular hydrogen from **11** is not accompanied by a reorganization of the remaining Ni-$(C_4H_5N)^+$ unit; in fact, the structural parameters of **11** and the product ion $Ni(C_4H_5N)^+$ are almost the same. Finally, an insertion of ethene in the Ni–N bond instead of the Ni–C bond as the first reaction step is also conceivable. However, while the formation of the cyclic product $Ni(CH_2CHNCHCH_2)^+$ and of H_2 are, according to the calculations, possible from a thermochemical point of view, this reaction path does not take place under thermal conditions because it is inhibited by a barrier of more than 100 kJ mol^{-1} (compared to the entrance channel). Selected bond lengths for all of the species given in Figure 4 are summarized in Table 2.

While the operation of a two-state reactivity (TSR) scenario is crucial in numerous reactions of cationic nickel complexes in the gas phase,[16,27] in the system described herein, according to the calculations it does not play a role. For example, as shown in Figure 3a, there is no need to invoke the involvement of an excited singlet state in the generation of the main product pair $CH_3CH{=}NH_2^+/^3Ni$. The reaction can smoothly proceed on the ground-state triplet surface. For the dehydrogenation reaction also (Figure 3b) a two-state reactivity scenario is not necessary because all intermediates, transition structures, and product pairs are for both states lower in energy as compared to the entrance channel. In the secondary reactions, the same situation prevails, and for the dehydrogenation [Equation (3)] a spin crossing does not need to be invoked. In fact, this would lead to an energetically quite demanding singlet $\mathbf{TS}_{10/11}$.

In summary, in this combined experimental/theoretical study we demonstrate that C–N bond formation in the couple $Ni(NH_2)^+/C_2H_4$ occurs efficiently under thermal conditions.[28] Further, the product ion $Ni(C_2H_4N)^+$ formed in the primary reaction undergoes a secondary reaction with another ethylene molecule, in which C–C bond making and breaking account for the generation of the product ions observed.

Experimental and Computational Section

The experiments were performed with a VG BIO-Q mass spectrometer of QHQ configuration (Q: quadrupole, H: hexapole) equipped with an ESI source as described in detail elsewhere.[29] Millimolar solutions of NiI_2 in formamide were introduced through a fused-silica capillary to the ESI source by a syringe pump (ca. 4 μL min^{-1}). As revealed by parent-ion scans, in which precursor ions can be identified, the $Ni(NH_2)^+$ cation is generated in the ESI source from dicationic $Ni(formamide)_3^{2+}$, as described previously for different systems.[12j,30] The degree of dissociation of the precursor ions owing to collisions with N_2, which is used as drying gas in the ESI source, is determined by the cone voltage; maximal yields of the desired complexes were achieved by adjusting the cone voltage to around 50–80 V. The identity of the ions was confirmed by comparison with the expected isotope patterns.[31] The ion/molecule reactions of the mass-selected cationic complexes with ethylene and its isotopologues were probed at a collision energy (E_{lab}) nominally set to 0 eV, which in conjunction with the circa 0.4 eV kinetic energy width of the parent ion at peak half height allows the investigation of quasi-thermal reactions, as demonstrated previously.[32] The error of the absolute rate coefficients is assumed to be ±50%. This error might be due to a different sensitivity of the gauge at different pressures. *E*- and *Z*-$C_2H_2D_2$ as well as C_2D_4 were purchased from CDN Isotopes Inc.; the purity is 99.7 atom% D for the $C_2H_2D_2$ isomers and 99.0 atom% for C_2D_4.

The DFT calculations, which aimed at obtaining a qualitative rather than a quantitative description, were performed with the Gaussian 09 program package[33] using the unrestricted B3LYP level of theory[34] and def2-QZVP basis sets.[35] While the B3LYP functional has been proven to be very useful in the performance of cost-efficient calculations of many molecular systems, however, it has also been found in some cases that B3LYP for example, overestimates bond energies quite substantially or does not reproduce correctly atomic

Table 2: Selected bond lengths (*r*), given in Å, of the species shown in Figure 4.[a]

	r(Ni-N)		*r*(Ni-C1)		*r*(C1-C2)		*r*(C2-C3)		*r*(C3-C4)		*r*(C4-N)	
2S+1	1	3	1	3	1	3	1	3	1	3	1	3
8	1.911	1.906	2.085	2.122	1.365	1.360	–	–	1.460	1.387	1.289	1.323
$\mathbf{TS}_{8/9}$	1.955	1.943	1.862	1.979	1.469	1.410	1.824	2.234	1.504	1.441	1.276	1.292
9	1.837	1.964	1.862	1.954	1.504	1.519	1.532	1.536	1.486	1.490	1.278	1.280
$\mathbf{TS}_{9/10}$	2.005	1.972	1.940	2.104	1.427	1.412	1.526	1.519	1.506	1.498	1.276	1.274
10	1.980	2.020	2.029	2.403	1.389	1.346	1.520	1.507	1.489	1.493	1.275	1.276
$\mathbf{TS}_{10/11}$	1.864	1.998	2.217	2.179	1.375	1.381	1.447	1.437	1.459	1.456	1.281	1.287
11	1.860	1.947	1.921	2.100	1.457	1.381	1.352	1.436	1.432	1.409	1.294	1.311
$Ni(C_4H_6N)^+$	1.815	1.926	1.859	2.043	1.465	1.396	1.346	1.424	1.435	1.416	1.292	1.309

[a] The numbering is based on $\mathbf{TS}_{8/9}$ where Ni is directly bound to C1; the following carbon atoms are numbered in ascending order ending with C4 which is bound to nitrogen.

states of transition-metal ions.[36] For example, the singlet/triplet splitting of Ni (13.5 kJ mol^{-1}) obtained by using B3LYP is lower than the experimental value of 40.8 kJ mol^{-1} [37] or the calculated BDE (Ni^+–NH_2) = 270 kJ mol^{-1} and BDE (Ni^+–C_2H_4) = 200 kJ mol^{-1} are overestimated by 37 or 18 kJ mol^{-1}, respectively, relative to the experimental data.[38] On the other hand, the comparison of the calculated and experimental proton affinities is quite good for Ni (736 kJ mol^{-1} vs. (737 ± 8) kJ mol^{-1}) and modest for C_2H_5N (910 kJ mol^{-1} vs. (885 ± 8) kJ mol^{-1}).[24] The performances of other functionals, for example the MO6 functional developed by Truhlar and Zhao,[39] were found to be comparable to B3LYP for the systems investigated in this study. To verify stationary points and transition states, frequency calculations were performed. All energies (given in kJ mol^{-1}) are corrected for (unscaled) zero-point vibrational energy contributions. Intrinsic reaction coordinate (IRC) calculations were performed to link transition structures with the corresponding minima.[40]

Received: June 27, 2011
Revised: November 28, 2011
Published online: February 10, 2012

Keywords: bond activation · C–C bond formation · C–N coupling · density functional calculations · nickel

[1] a) *Comprehensive Natural Products Chemistry*, *Vol.* 4 (Eds.: D. H. R. Barton, K. Nakanishi, O. Meth-Cohn), Elsevier, Oxford, **1999**; b) A. Ricci, *Modern Amination Methods*, Wiley-VCH, Weinheim, **2000**; c) A. Ricci, *Amino Group Chemistry*: *From Synthesis to the Life Science*, Wiley-VCH, Weinheim, **2008**.

[2] a) D. Steinborn, R. Taube, *Z. Chem.* **1986**, *26*, 349 – 359; b) T. E. Müller, M. Beller, *Chem. Rev.* **1998**, *98*, 675 – 703; c) R. Taube in *Applied Homogenous Catalysis with Organometallic Compounds*, *Vol. 1* (Ed.: B. Cornils, W. A. Herrmann), Wiley-VCH, Weinheim, **1997**, pp. 507 – 520; d) J. J. Brunet, D. Neibecker in *Catalytic Heterofunctionalization from Hydroamination to Hydrozirconation* (Eds.: A. Togni, H. Grützmacher), Wiley-VCH, Weinheim, **2001**, pp. 91 – 141; e) T. E. Müller, K. C. Hultzsch, M. Yus, F. Foubelo, M. Tada, *Chem. Rev.* **2008**, *108*, 3795 – 3892; f) J. L. Klinkenberg, J. F. Hartwig, *Angew. Chem.* **2011**, *123*, 88 – 98; *Angew. Chem. Int. Ed.* **2011**, *50*, 86 – 95.

[3] E. Haak, S. Doye, *Chem. Unserer Zeit* **1999**, *33*, 296 – 303.

[4] R. Hoffmann, R. B. Woodward, *Science* **1970**, *167*, 825 – 831.

[5] a) D. M. Roundhill, *Chem. Rev.* **1992**, *92*, 1 – 27; b) D. M. Roundhill, *Catal. Today* **1997**, *37*, 155 – 165; c) M. Nobis, B. Driessen-Holscher, *Angew. Chem.* **2001**, *113*, 4105 – 4108; *Angew. Chem. Int. Ed.* **2001**, *40*, 3983 – 3985; d) P. W. Roesky, T. E. Müller, *Angew. Chem.* **2003**, *115*, 2812 – 2814; *Angew. Chem. Int. Ed.* **2003**, *42*, 2708 – 2710; e) M. Beller, J. Seayad, A. Tillack, H. Jiao, *Angew. Chem.* **2004**, *116*, 3448 – 3479; *Angew. Chem. Int. Ed.* **2004**, *43*, 3368 – 3398; f) J. F. Hartwig, *Pure Appl. Chem.* **2004**, *76*, 507 – 516; g) K. C. Hultzsch, *Adv. Synth. Catal.* **2005**, *347*, 367 – 391; h) J.-J. Brunet, N.-C. Chu, M. Rodriguez-Zubiri, *Eur. J. Inorg. Chem.* **2007**, 4711 – 4722; i) J. F. Hartwig, *Nature* **2008**, *455*, 314 – 322; j) K. D. Hesp, M. Stradiotto, *ChemCatChem* **2010**, *2*, 1192 – 1207.

[6] J. F. Hartwig in *Organotransition Metal Chemistry*: *From Bonding to Catalysis*, University Science Book, Sausalito, **2010**, pp. 700 – 717.

[7] a) G. P. Pez, J. E. Galle, *Pure Appl. Chem.* **1985**, *57*, 1917 – 1926; b) M. Beller, C. Breindl, *Tetrahedron* **1998**, *54*, 6359 – 6368; c) M. Beller, C. Breindl, T. H. Riermeier, M. Eichberger, H. Trauthwein, *Angew. Chem.* **1998**, *110*, 3571 – 3573; *Angew. Chem. Int. Ed.* **1998**, *37*, 3389 – 3391.

[8] a) A. L. Casalnuovo, J. C. Calabrese, D. Milstein, *J. Am. Chem. Soc.* **1988**, *110*, 6738 – 6744; b) R. Dorta, P. Egli, F. Zürcher, A. Togni, *J. Am. Chem. Soc.* **1997**, *119*, 10857 – 10858; c) D. M. Gardner, R. T. Clark, US4.454.321, **1984** [*Chem. Abstr.* **1984**, *101*, 130217r]; d) M. Beller, H. Trauthwein, M. Eichberger, C. Breindl, J. Herwig, T. E. Müller, O. R. Thiel, *Chem. Eur. J.* **1999**, *5*, 1306 – 1319; e) V. Lavallo, G. D. Frey, B. Donnadieu, M. Soleilhavoup, G. Bertrand, *Angew. Chem.* **2008**, *120*, 5302 – 5306; *Angew. Chem. Int. Ed.* **2008**, *47*, 5224 – 5228.

[9] a) M. R. Gagné, L. Brard, V. P. Conticello, M. A. Giardello, C. L. Stern, T. J. Marks, *Organometallics* **1992**, *11*, 2003 – 2005; b) M. A. Giardello, V. P. Conticello, L. Brard, M. R. Gagné, T. J. Marks, *J. Am. Chem. Soc.* **1994**, *116*, 10241 – 10254; c) Y. W. Li, T. J. Marks, *Organometallics* **1996**, *15*, 3770 – 3772; d) S. Hong, T. J. Marks, *Acc. Chem. Res.* **2004**, *37*, 673 – 686.

[10] A. L. Reznichenko, H. N. Nguyen, K. C. Hultzsch, *Angew. Chem.* **2010**, *122*, 9168 – 9171; *Angew. Chem. Int. Ed.* **2010**, *49*, 8984 – 8987.

[11] T. Hamann, E. Böhler, P. Swiderek, *Angew. Chem.* **2009**, *121*, 4715 – 4718; *Angew. Chem. Int. Ed.* **2009**, *48*, 4643 – 4645.

[12] a) S. W. Buckner, J. R. Gord, B. S. Freiser, *J. Am. Chem. Soc.* **1988**, *110*, 6606 – 6612; b) D. F. A. Ranatunga, Y. D. Hill, B. S. Freiser, *Organometallics* **1996**, *15*, 1242 – 1250; c) M. Brönstrup, I. Kretzschmar, D. Schröder, H. Schwarz, *Helv. Chim. Acta* **1998**, *81*, 2348 – 2369; d) M. Aschi, M. Brönstrup, M. Diefenbach, J. N. Harvey, D. Schröder, H. Schwarz, *Angew. Chem.* **1998**, *110*, 858 – 861; *Angew. Chem. Int. Ed.* **1998**, *37*, 829 – 832; e) M. Diefenbach, M. Brönstrup, M. Aschi, D. Schröder, H. Schwarz, *J. Am. Chem. Soc.* **1999**, *121*, 10614 – 10625; f) K. Koszinowski, D. Schröder, H. Schwarz, *J. Am. Chem. Soc.* **2003**, *125*, 3676 – 3677; g) K. Koszinowski, D. Schröder, H. Schwarz, *Organometallics* **2003**, *22*, 3809 – 3819; h) K. Koszinowski, D. Schröder, H. Schwarz, *Organometallics* **2004**, *23*, 1132 – 1139; i) K. Koszinowski, D. Schröder, H. Schwarz, *Angew. Chem.* **2004**, *116*, 124 – 127; *Angew. Chem. Int. Ed.* **2004**, *43*, 121 – 124; j) R. Kretschmer, M. Schlangen, H. Schwarz, *Angew. Chem.* **2011**, *123*, 5499 – 5503; *Angew. Chem. Int. Ed.* **2011**, *50*, 5387 – 5391; k) for a recent review, see: R. Kretschmer, M. Schlangen, H. Schwarz, *Chem. Eur. J.* **2012**, *18*, 40 – 49, and references therein.

[13] a) H. Schwarz, *Chem. Unserer Zeit* **1991**, *25*, 268 – 278; b) D. K. Böhme, H. Schwarz, *Angew. Chem.* **2005**, *117*, 2388 – 2406; *Angew. Chem. Int. Ed.* **2005**, *44*, 2336 – 2354; c) H. Schwarz, *Angew. Chem.* **2011**, *123*, 10276 – 10297; *Angew. Chem. Int. Ed.* **2011**, *50*, 10096 – 10115.

[14] R. Kretschmer, M. Schlangen, H. Schwarz, unpublished results.

[15] For details of the $Ni(NH_2)^+$ formation, see the Experimental Section.

[16] For a review, see: M. Schlangen, H. Schwarz, *J. Catal.* **2011**, *284*, 126 – 137 and references therein.

[17] a) *Metal Ions in Life Science—Nickel and its Surprising Impact in Nature*, Vol. 2 (Eds.: A. Sigel, H. Sigel, R. K. O. Sigel), Wiley, Chichester, **2007**; b) An entire issue of Tetrahedron is devoted to modern, nickel-based catalysis; see: T. F. Jamison, *Tetrahedron* **2006**, *62*, 7503 – 7610.

[18] The branching ratio was determined by extrapolating the pressure of ethene to zero.

[19] a) The absolute rate coefficient for the reaction cannot be measured directly in our multipole set-up; rather, the rate coefficient was determined by using the Pt^+/CH_4 system as a reference: D. Schröder, H. Schwarz, *Can. J. Chem.* **2005**, *83*, 1936 – 1940 and references therein; b) collision-rate calculations (G. Gioumousis, D. P. Stevenson, *J. Chem. Phys.* **1958**, *29*, 294 – 299) were performed by using the method of Langevin: M. P. Langevin, *Ann. Chim. Phys.* **1905**, *8*, 245 – 288.

[20] a) B. H. Solka, M. E. Russell, *J. Phys. Chem.* **1974**, *78*, 1268 – 1273; b) K. Levsen, F. W. Mclaffer, *J. Am. Chem. Soc.* **1974**, *96*, 139 – 144; c) F. Jordan, *J. Phys. Chem.* **1976**, *80*, 76 – 82; d) R. D. Bowen, D. H. Williams, G. Hvistendahl, *J. Am. Chem. Soc.* **1977**, *99*, 7509 – 7515; e) V. Barone, F. Lelj, P. Grande, N. Russo, *J. Mol.*

Struct. THEOCHEM **1985**, *124*, 319 – 324; f) J. Henriksen, S. Hammerum, *Int. J. Mass Spectrom.* **1998**, *179 – 180*, 301 – 308.
[21] J. I. van der Vlugt, *Chem. Soc. Rev.* **2010**, *39*, 2302 – 2322.
[22] Unfortunately, as $Ni(ND_2)^+$ is isobaric with $Ni(OD)^+$, and as the resolving power of the instrument is not high enough for a proper mass separation, labeling experiments with $Ni(ND_2)^+$ were not performed.
[23] B. Åkermark, M. Almemark, J. Almlöf, J. E. Bäckvall, B. Roos, Å. Støgard, *J. Am. Chem. Soc.* **1977**, *99*, 4617 – 4624.
[24] E. P. L. Hunter, S. G. Lias, *J. Phys. Chem. Ref. Data* **1998**, *27*, 413 – 656.
[25] a) F. Sette, J. Stohr, A. P. Hitchcock, *J. Chem. Phys.* **1984**, *81*, 4906 – 4914; b) X. Q. Lu, W. Y. Guo, T. F. Yang, L. M. Zhao, S. C. Du, L. Wang, H. H. Shan, *J. Phys. Chem. A* **2008**, *112*, 5312 – 5321.
[26] The numbering of the carbon-atom skeleton is described in footnote[a] of Tables 1 and 2.
[27] a) D. Schröder, S. Shaik, H. Schwarz, *Acc. Chem. Res.* **2000**, *33*, 139 – 145; b) Q. Zhang, M. T. Bowers, *J. Phys. Chem. A* **2004**, *108*, 9755 – 9761; c) M. Schlangen, H. Schwarz, *Angew. Chem.* **2007**, *119*, 5711 – 5715; *Angew. Chem. Int. Ed.* **2007**, *46*, 5614 – 5617.
[28] It should be noted that in the thermal reaction of $Fe(NH_2)(CH_3)^+$ with C_2H_4, no C–N bond coupling occurs; rather, insertion of the olefin in the Fe–C bond of the cation takes place. For details, see: S. Karrass, D. Stöckigt, D. Schröder, H. Schwarz, *Organometallics* **1993**, *12*, 1449 – 1452.
[29] C. Trage, D. Schröder, H. Schwarz, *Chem. Eur. J.* **2005**, *11*, 619 – 627.
[30] T. J. Shi, K. W. M. Siu, A. C. Hopkins, *Int. J. Mass Spectrom.* **2006**, *255*, 251 – 264.
[31] Scientific Instrument Services: Isotope distribution calculator and mass spectrum plotter: http://www.sisweb.com/mstools/isotope.htm, accessed Nov 23, **2011**.
[32] a) D. Schröder, H. Schwarz, S. Schenk, E. Anders, *Angew. Chem.* **2003**, *115*, 5241 – 5244; *Angew. Chem. Int. Ed.* **2003**, *42*, 5087 – 5090; b) C. Trage, M. Diefenbach, D. Schröder, H. Schwarz, *Chem. Eur. J.* **2006**, *12*, 2454 – 2464; c) D. Schröder, M. Engeser, H. Schwarz, E. C. E. Rosenthal, J. Döbler, J. Sauer, *Inorg. Chem.* **2006**, *45*, 6235 – 6245; d) P. Gruene, C. Trage, D. Schröder, H. Schwarz, *Eur. J. Inorg. Chem.* **2006**, 4546 – 4552.
[33] *G*aussian 09 (Revision A.1), M. J. Frisch, G. W. Trucks, H. B. Schlegel, G. E. Scuseria, M. A. Robb, J. R. Cheeseman, G. Scalmani, V. Barone, B. Mennucci, G. A. Petersson, H. Nakatsuji, M. Caricato, X. Li, H. P. Hratchian, A. F. Izmaylov, J. Bloino, G. Zheng, J. L. Sonnenberg, M. Hada, M. Ehara, K. Toyota, R. Fukuda, J. Hasegawa, M. Ishida, T. Nakajima, Y. Honda, O. Kitao, H. Nakai, T. Vreven, J. Montgomery, J. A., J. E. Peralta, F. Ogliaro, M. Bearpark, J. J. Heyd, E. Brothers, K. N. Kudin, V. N. Staroverov, R. Kobayashi, J. Normand, K. Raghavachari, A. Rendell, J. C. Burant, S. S. Iyengar, J. Tomasi, M. Cossi, N. Rega, N. J. Millam, M. Klene, J. E. Knox, J. B. Cross, V. Bakken, C. Adamo, J. Jaramillo, R. Gomperts, R. E. Stratmann, O. Yazyev, A. J. Austin, R. Cammi, C. Pomelli, J. W. Ochterski, R. L. Martin, K. Morokuma, V. G. Zakrzewski, G. A. Voth, P. Salvador, J. J. Dannenberg, S. Dapprich, A. D. Daniels, Ö. Farkas, J. B. Foresman, J. V. Ortiz, J. Cioslowski, D. J. Fox, Gaussian Inc. Wallingford CT, **2009**.
[34] a) C. Lee, W. Yang, R. G. Parr, *Phys. Rev. B* **1988**, *37*, 785 – 789; b) A. D. Becke, *J. Chem. Phys.* **1993**, *98*, 5648 – 5652.
[35] F. Weigend, R. Ahlrichs, *Phys. Chem. Chem. Phys.* **2005**, *7*, 3297 – 3305.
[36] a) Y. Zhao, N. Gonzalez-Garcia, D. G. Truhlar, *J. Phys. Chem. A* **2005**, *109*, 2012 – 2018; b) Y. Zhao, D. G. Truhlar, *Acc. Chem. Res.* **2008**, *41*, 157 – 167.
[37] http://webbook.nist.gov/chemistry.
[38] a) D. E. Clemmer, P. B. Armentrout, *J. Phys. Chem.* **1991**, *95*, 3084 – 3090; b) M. R. Sievers, L. M. Jarvis, P. B. Armentrout, *J. Am. Chem. Soc.* **1998**, *120*, 1891 – 1899.
[39] Y. Zhao, D. G. Truhlar, *Theor. Chem. Acc.* **2008**, *120*, 215 – 241.
[40] a) K. Fukui, *J. Phys. Chem.* **1970**, *74*, 4161 – 4163; b) K. Fukui, *Acc. Chem. Res.* **1981**, *14*, 363 – 368; c) C. Gonzalez, H. B. Schlegel, *J. Phys. Chem.* **1990**, *94*, 5523 – 5527; d) D. G. Truhlar, M. S. Gordon, *Science* **1990**, *249*, 491 – 498.

